

## Large compact clusters and fast dynamics in coupled nonequilibrium systems

Shaury Chakraborty,<sup>1</sup> Sukla Pal,<sup>1</sup> Sakuntala Chatterjee,<sup>1,\*</sup> and Mustansir Barma<sup>2</sup>

<sup>1</sup>*Department of Theoretical Sciences, S.N. Bose National Centre for Basic Sciences, Block-JD, Sector-III, Salt Lake, Kolkata 700098, India*

<sup>2</sup>*TIFR Centre for Interdisciplinary Sciences, 21 Brundavan Colony, Osman Sagar Road, Narsingi, Hyderabad 500075, India*

(Received 10 March 2016; published 16 May 2016)

We demonstrate particle clustering on macroscopic scales in a coupled nonequilibrium system where two species of particles are advected by a fluctuating landscape and modify the landscape in the process. The phase diagram generated by varying the particle-landscape coupling, valid for all particle densities and in both one and two dimensions, shows novel nonequilibrium phases. While particle species are completely phase separated, the landscape develops macroscopically ordered regions coexisting with a disordered region, resulting in coarsening and steady state dynamics on time scales which grow algebraically with size, not seen earlier in systems with pure domains.

DOI: [10.1103/PhysRevE.93.050102](https://doi.org/10.1103/PhysRevE.93.050102)

Particle clustering is important in many natural physical and biological phenomena, for instance, the formation of sediments [1] and protein clustering on a biological membrane [2]. Evidently, it is important to understand processes that cause clustering in different physical contexts, and how these processes influence the properties of the cluster and the time taken to form it. Often, large-scale clustering is driven by interactions with an external medium which itself has correlations in space and time [3–5]. An important physical effect in such systems is the back influence of the particles on the medium. This interaction can aid clustering, or destroy it. If a cluster does form, it may be compact and robust, or a dynamic object that undergoes constant reorganization. The formation time may grow exponentially with the size, or as a power law. Given this wealth of possibilities, it is important to look for an understanding, within simple models, of the circumstances under which different sorts of macroscopically clustered states occur.

In this Rapid Communication, we derive the phase diagram of a simple model system as we vary the interaction between the environment and particles. In the process, we unmask a novel nonequilibrium phase of particles with compact clustering and rich and rapid dynamics coexisting with a macroscopically organized landscape. The model has partial overlap with the lattice gas model of Lahiri and Ramaswamy (LR) for sedimenting colloidal crystals [6,7], but the new phases manifest themselves outside the LR regime. Our results hold in both one and two dimensions.

The model consists of two sets of particles moving stochastically in a fluctuating potential energy landscape. Particles try to minimize their energy by (a) moving along the local potential gradient of the landscape and (b) modifying the landscape around them in such a way as to lower the energy further. The model is generic but we discuss it in the language of particles confined to move on a fluctuating surface in the presence of gravity, where the particles can locally distort the surface shape to further lower the energy (see Fig. 1). One of the particle species is considered lighter and the other is heavier; we use the name LH (light-heavy) model to describe the system. Process (b) affects the landscape dynamics quite

differently in parts which are rich or poor in one species of particle, ultimately resulting in the formation of distinct macroscopic regions, each corresponding to a phase. Our study reveals a rich set of phenomena: strong phase separation with fluctuationless phases for particles, but a different sort of organization for the landscape; a rapid approach to the steady state; and intricate steady state dynamics of the interfaces between phases, with three distinct temporal regimes.

There has been a recent surge of activity in the field of coupled driven diffusive systems [8–10], and it is useful to view our work in this context. This activity has resulted in a catalog of universality classes which describe how propagating modes in these systems decay in time. The modes themselves are defined by diagonalizing coupled hydrodynamic equations to linear order, with eigenvalues giving their speeds of propagation. The disordered phase of our system is indeed described by this theory. But the ordered phases of primary interest to us correspond to *complex* eigenvalues at the linear level [11]; the imaginary parts signal instabilities, heralding macroscopic phase separation. However, such linear analysis cannot reveal the characteristics of the final phases, which can and do differ from each other in fundamental respects. Our results provide the necessary characterization and thus contribute to the important goal of classifying ordered phases in coupled driven diffusive systems.

In a nutshell, the quintessentially nonequilibrium states found here exhibit phase separation, with qualitatively different types of ordering for the particles and landscape, quite unlike systems known earlier. In particular, particles display strong phase separation [7] characterized by pure, fluctuationless phases, which cohabit with three macroscopic regions of the surface, two of which possess long-range order, while the third does not. These findings differ markedly from the strongly phase separated states found earlier in the LR and *ABC* models [7,12] and imply strong changes for both static and dynamical properties. Notably, the approach to our steady state is rapid, with a coarsening time that grows as a power law of size, as opposed to the much slower exponentially growing time scales found earlier.

The LH model consists of two coupled driven diffusive systems, with conserved quantities. This is a lattice model of *H* (heavier) and *L* (lighter) particles with damped motion under gravity and residing on a fluctuating surface. The local

\*sakuntala.chatterjee@bose.res.in

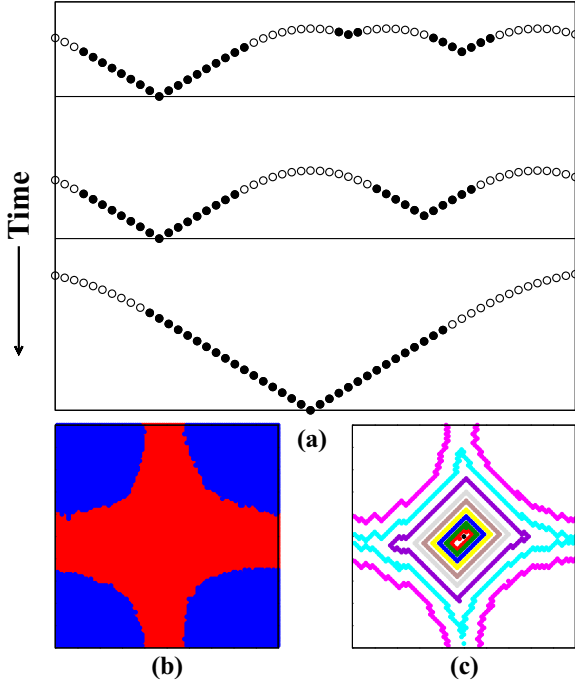


FIG. 1. Schematic presentation of different phases in one and two dimensions. (a) shows the coarsening mechanism in one dimension for  $b' \leq 0$ .  $H$  ( $L$ ) particles are shown by solid (open) circles. (b) and (c) show typical configurations in two dimensions. In (b) the  $H$  ( $L$ ) cluster is shown in red (blue) and (c) shows the equal height contours.

dynamics of the particles and the surface are coupled:  $H$  and  $L$  particles at neighboring sites may interchange locations, and do so preferentially if the local tilt of the surface favors a downward move for  $H$ . Particles reside on lattice sites and interact via hard-core exclusion: a site holds at most one particle ( $H$  or  $L$ ). If the symbols  $/$  and  $\backslash$  indicate upward and downward tilts of the surface, respectively, then the particles follow the dynamics:

$$\begin{aligned} W(H \backslash L \rightarrow L \backslash H) &= D + a, \\ W(L \backslash H \rightarrow H \backslash L) &= D - a, \\ W(H / L \rightarrow L / H) &= D - a, \\ W(L / H \rightarrow H / L) &= D + a, \end{aligned} \quad (1)$$

where  $W$  denotes the probability per unit time for a particular process to occur. This dynamics conserves the total number of  $H$  (and  $L$ ) particles. Under the weight of the particles, a local hill on the surface gets pushed downward, at a higher rate by  $H$  than by  $L$ . In one dimension, the surface consists of a chain with  $N$  sites. The lattice bonds representing discrete surface elements, can have two possible orientations with slopes  $\tau_{i+1/2} = \pm 1$ , which are called upslope and downslope bonds, respectively. In one dimension surface dynamics can be represented as

$$\begin{aligned} W(/H \backslash \rightarrow \backslash H /) &= E + b, \\ W(\backslash H / \rightarrow / H \backslash) &= E - b, \\ W(/L \backslash \rightarrow \backslash L /) &= E - b', \\ W(\backslash L / \rightarrow / L \backslash) &= E + b'. \end{aligned} \quad (2)$$

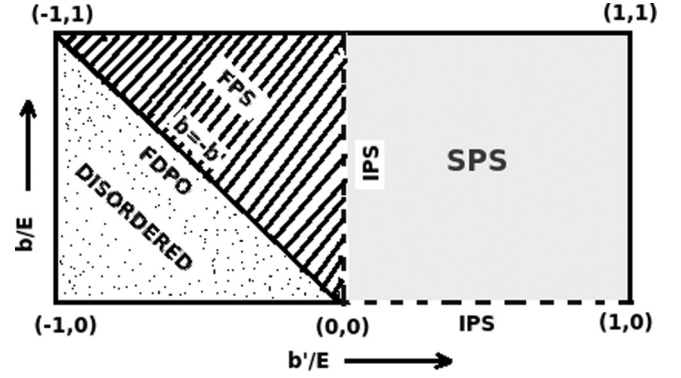


FIG. 2. Phase diagram in the  $b$ - $b'$  plane. For  $b > 0$  and  $b' > 0$ , the system shows SPS. The dotted horizontal and vertical lines are related to each other via interchange of the two particle species. On these lines the system is in IPS phase. The striped region ( $-b < b' < 0$ ) represents the FPS phase. The  $b = -b'$  line corresponds to the FDPO phase. The dotted region ( $b' < -b$ ) corresponds to the disordered phase.

This dynamics conserves the overall slope. In two dimensions the surface consists of a square lattice and the height of a site can change, provided all four neighboring sites are at the same height [13,14]. We consider periodic boundary conditions with no overall tilt of the surface.

Figure 2 shows the phase diagram of the system in the  $bb'$  plane, with  $a$  taken to be positive. It follows from Eq. (2) that interchanging  $b$  and  $b'$  is tantamount to interchanging the  $H$  and  $L$  species. Hence we consider positive  $b$ , while  $b'$  can be positive or negative or zero.

**Strong phase separation (SPS):** The right half of the phase diagram,  $b' > 0$ , corresponds to the LR model [6,7], as appropriate to sedimenting colloidal crystals [6]. In this regime, the light particles tend to move the surface upward. In steady state, the upslope and downslope surface bonds phase separate to form a single macroscopic valley and hill, which hold all the  $H$  and  $L$  particles, respectively, in separated clusters. Both particles and tilts show SPS; the approach to steady state is extremely slow [involving times  $T_{\text{relax}} \sim \exp(\alpha N)$ ] owing to the formation of large metastable barriers.

In the left half of the phase diagram in Fig. 2 we have  $b' < 0$ , which means that the part of the surface occupied by  $L$  particles shows a downward drift. As discussed below, different phases are obtained depending on whether this velocity is larger than, smaller than, or the same as the velocity imparted by the  $H$  particles.

**Disordered phase:** When the  $L$  particles push the surface faster (dotted region in Fig. 2), neither of the particle species nor the tilts shows long-range order. Interesting dynamical aspects of this wave-carrying disordered phase will be presented elsewhere [15].

**Fluctuation-dominated phase ordering (FDPO):** On the line  $b = -b'$ , both  $L$  and  $H$  particles push the landscape down at the same rate. This implies Kardar-Parisi-Zhang dynamics for the surface while  $L$ - $H$  exchange rules [Eq. (1)] imply that  $H$  particles tend to collect in local valleys. This reduces to the passive scalar problem studied earlier, in which particles exhibit FDPO, characterized by singularities of the two-point

correlations and giant fluctuations of the density [16,17]. Interestingly, this phase boundary can be identified exactly by looking for the onset of complex eigenvalues in a linear stability analysis of the coupled hydrodynamic equations for the landscape and the particles [14].

*Fast fall with phase separation (FPS):* When  $L$  particles push the surface down at a slower rate than  $H$ 's, a new phase ensues (shown striped in Fig. 2). In steady state,  $L$  and  $H$  particles separate completely as in SPS. The surface underlying the  $H$  cluster forms a macroscopic valley but unlike SPS, the phases are not pure, e.g., the macroscopic majority-upslope region accommodates a finite fraction  $(1 - m)$  of downslope bonds. The majority-upslope region in turn acts as a 'tilt reservoir' which drives a finite tilt current through the part of the surface which holds  $L$  particles. By identifying an upslope (downslope) bond with a particle (hole) we identify the phase as the maximal current phase in an open-chain asymmetric exclusion process [14,18]. Consequently, near the edges of the  $L$  domain the tilt density  $\rho$  shows an algebraic  $1/\sqrt{r}$  variation, while in the bulk  $\rho \approx 1/2$  [14]. Equating the tilt current  $J = 2bm(1 - m)$  in the two arms holding the  $H$  particles with that in the maximal current phase  $J' = 2b'/4$  in the  $L$ -rich portion, we deduce  $4m(1 - m) = b'/b$ , a relation we have verified numerically. The presence of a finite tilt current through the system results in a finite downward velocity of the surface and in steady state, the full surface moves downward at finite speed, preserving the macroscopic valley and disordered tilt region, along with the pure domains of  $H$  and  $L$  particles [Fig. 1(a)].

*Infinitesimal fall with phase separation (IPS):* For  $b' = 0$  (the vertical dashed line in Fig. 2) the local fluctuations in the surface occupied by  $L$  particles are of the symmetric Edwards-Wilkinson type. In this phase, the  $H$  and  $L$  particles again form pure domains. The surface beneath the  $H$  cluster has the shape of a deep valley consisting of pure domains of upslope and downslope bonds. By contrast, the surface occupied by the cluster in this case behaves like an open-chain symmetric exclusion process connected to the two reservoirs of upslope and downslope tilts at the two ends. Thus the tilt density varies linearly in this region with a gradient  $\sim 1/N$  [14,19], leading to a tilt current and an infinitesimal downward velocity  $\sim 1/N$  of the entire landscape. We schematically show a typical configuration in Fig. 1(a).

The general properties of the phases discussed above remain valid even in two dimensions, where  $H$  and  $L$  particles form compact clusters. The shape of these two dimensional clusters depends on the topography of the surface heights. As in one dimension, we find a deep valley that holds the  $H$  cluster. Measured from the bottommost point, the height increases linearly in both  $x$  and  $y$  directions and it is easy to see that in this case the equal height contours have the shape of a diamond. In Figs. 1(b) and 1(c), we show some representative configurations.

The way in which the landscape is organized in the IPS and FPS phases has a profound influence on dynamical properties. For instance, although the center of mass of the  $H$  cluster remains stationary for a long time, the landscape immediately below it undulates in time, leading to three distinct temporal regimes in steady state. These are captured by monitoring the mean-squared displacement  $\sigma^2$  of the deepest point of the valley. Figure 3 presents the data for  $b' = 0$ . At small time

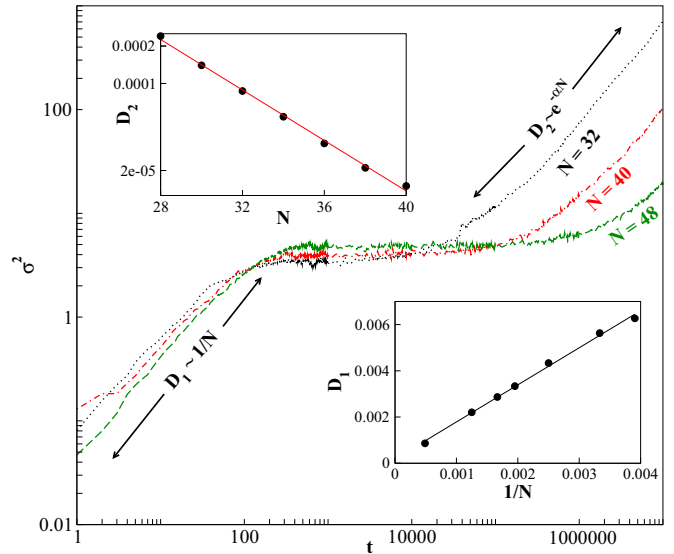


FIG. 3. Occurrence of three regimes in the steady state dynamics of the deepest point of the valley. Main plot: Mean squared displacement of the deepest point of the valley as a function of time. The displacement shows an initial diffusive growth, followed by a plateau, and finally another diffusive regime at large time. Bottom inset: Small time diffusivity  $D_1 \sim 1/N$ . Top inset: For large time, the diffusivity  $D_2 \sim e^{-\alpha N}$ , with  $\alpha \simeq 0.26$ . These data correspond to  $b' = 0$ ,  $b = E$ ,  $a = D$  and have been averaged over 5000 steady state configurations.

$t \ll N^2$ , we find  $\sigma^2$  grows diffusively with a diffusion constant  $D_1 \sim 1/N$ . But after times of order  $N^2$ , a plateau for  $\sigma^2$  is reached at a value  $\sim N$ . From a simple consideration of the total (gravitational) energy of the  $H$  particles, it is easy to show that when the deepest point coincides with the center of mass of the  $H$  cluster, the energy is minimum. Any displacement from this position gives rise to a restoring force that scales linearly with the displacement. The motion of the deepest point is thus described by an Ornstein-Uhlenbeck process [20]; consequently, the deepest point diffuses within a region of size  $\sqrt{N}$  around the  $H$  cluster center of mass [14]. Finally, at very large  $t$ , the  $H$  cluster itself moves diffusively around the system and the valley moves along with it (see [14]). The mean-squared displacement of the deepest point in this regime has a diffusion coefficient  $D_2 \sim e^{-\alpha N}$ .

Another important aspect of the dynamics concerns the relaxation to steady state starting from an initially disordered state. Interestingly, IPS and FPS phases show an enormous reduction in this relaxation time, as compared to earlier known examples of SPS as in the LR and ABC models [7,12]. For  $b' > 0$  (LR model), the landscape occupied by an  $L$  cluster tends to move upwards and forms a hill, while an  $H$  cluster pushes the landscape down and forms a valley. For two adjacent valleys with  $H$  clusters to merge, the time to dissolve the intermediate hill containing the  $L$  cluster grows exponentially with the size of the  $L$  cluster, and hence the final SPS state is reached over a time scale  $e^{\gamma N}$ . By contrast, in the FPS and IPS ( $b' \leq 0$ ) phases, the landscape is organized differently, and this leads to fast relaxation, with times growing as  $N^2$ . This is because the part of the landscape beneath the intervening

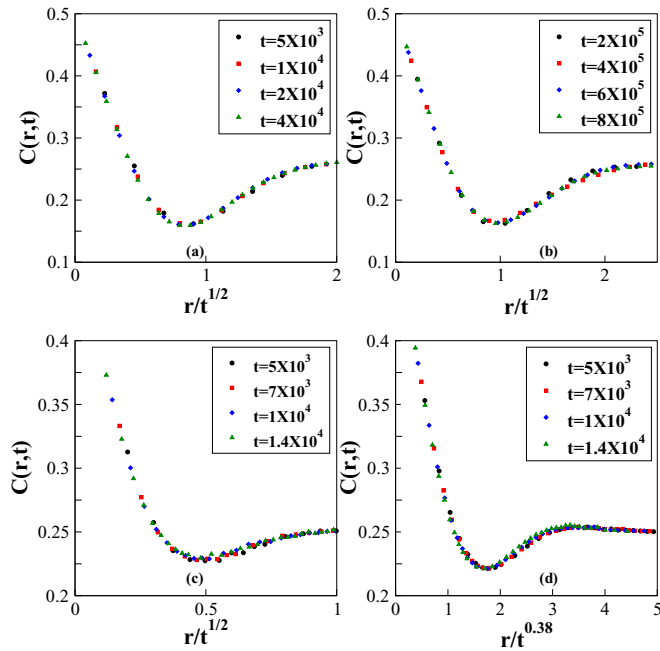


FIG. 4. Scaling of particle density correlation in the coarsening phase in both one and two dimensions. The equal time density correlation for the particles  $C(r,t)$  shows a collapse when  $r$  is scaled by  $\mathcal{L}(t) \sim t^{1/z}$ . (a) and (c) show scaled data for  $b = 0.5$ ,  $b' = 0$  in one and two dimensions, respectively. Here we find  $z \simeq 2$ . (b) and (d) show similar plots for  $b = 0.3$ ,  $b' = -0.2$ . Here, in one dimension,  $z \simeq 2$  and in two dimensions  $z \simeq 2.6$ . We have used  $N = 1024$  (a),  $N = 16384$  (b), and  $N = 256 \times 256$  [(c) and (d)] here.

$L$  cluster either shows symmetric fluctuations (for  $b' = 0$ ) or gets pushed downward (for  $b' < 0$ ). Figure 4 shows the scaling collapse of the equal time density correlation function for  $H$  particles when separations are scaled by the coarsening length scale  $\mathcal{L}(t)$ , which is found to grow as  $t^{1/z}$ . In IPS phase ( $b' = 0$ ) we find  $z = 2$  in both one and two dimensions. The FPS phase ( $-b < b' < 0$ ) shows  $z \simeq 2$  in one dimension for very large

$N$  and  $t$ , while for smaller values of these variables, our data show finite size effects (see [14] for details). In two dimensions for FPS, we measured  $z \simeq 2.6$ , for the largest values of  $N$  and  $t$  we could access. Our plots in Fig. 4 demonstrate algebraic coarsening for completely phase-separated systems, and stand in strong contrast to the ultraslow logarithmic coarsening observed in the LR and *ABC* models [7,12]. Underlying the speedup of the coarsening process is a simple mechanism, namely, the formation of disordered segments of the landscape between ordered clusters. These segments generate fluctuations which allow mergers of ordered regions to occur on a rapid time scale.

To summarize, we have considered coupled driven systems consisting of two species of particles being advected by an energy landscape whose dynamics is in turn influenced by the particles. The differential interaction between the landscape and the two particle species gives rise to different phases in the system as the interaction parameters are varied. We have demonstrated the occurrence of new phases with fast dynamics, where both the particles and the landscape show long-range order and the composite system is in a nonequilibrium current-carrying state.

We conclude with a discussion of the implications of our work for modeling in biophysical contexts. It is known that on the cell membrane, various proteins, and lipids like integrins, T-cell receptors are present in the form of nanoclusters [21,22]. This clustering is shown to be induced by the cortical actin cytoskeleton [2,23], and within a recent theoretical model of the process, an FDPO state has been observed [24]. There is now experimental evidence that the actin cytoskeleton also gets reorganized by these membrane components [22,25]. This raises the interesting possibility of new phases arising if the treatment of [24] is extended to account for the back action of membrane components on the cytoskeleton.

*Acknowledgments.* We acknowledge useful discussions with T. Sadhu, M. Rao, and A. Das. The computational facility used in this work was provided through Thematic Unit of Excellence on Computational Materials Science, funded by Nanomission, Department of Science and Technology (India).

- [1] S. Ramaswamy, *Adv. Phys.* **50**, 297 (2001).
- [2] K. Gowrishankar, S. Ghosh, S. Saha, C. Rumamol, S. Mayor, and M. Rao, *Cell* **149**, 1353 (2012).
- [3] J. M. Deutsch, *J. Phys. A* **18**, 1449 (1985).
- [4] M. Wilkinson and B. Mehlig, *Phys. Rev. E* **68**, 040101 (2003).
- [5] B. Drossel and M. Kardar, *Phys. Rev. Lett.* **85**, 614 (2000); A. Nagar, M. Barma, and S. N. Majumdar, *ibid.* **94**, 240601 (2005).
- [6] R. Lahiri and S. Ramaswamy, *Phys. Rev. Lett.* **79**, 1150 (1997).
- [7] R. Lahiri, M. Barma, and S. Ramaswamy, *Phys. Rev. E* **61**, 1648 (2000).
- [8] H. van Beijeren, *Phys. Rev. Lett.* **108**, 180601 (2012).
- [9] P. Ferrari, S. Sasamoto, and H. Spohn, *J. Stat. Phys.* **153**, 377 (2013).
- [10] V. Popkov, A. Schadschneider, J. Schmidt, and G. Schütz, *Proc. Natl. Acad. Sci. USA* **112**, 12645 (2015).
- [11] S. Ramaswamy, M. Barma, D. Das, and A. Basu, *Phase Transit.* **75**, 363 (2002).
- [12] M. R. Evans, Y. Kafri, H. M. Koduvally, and D. Mukamel, *Phys. Rev. Lett.* **80**, 425 (1998).
- [13] G. Manoj and M. Barma, *J. Stat. Phys.* **110**, 1305 (2013).
- [14] See Supplemental Material at <http://link.aps.org/supplemental/10.1103/PhysRevE.93.050102> for details of calculations and additional data from simulations.
- [15] S. Chakraborty, S. Chatterjee, and M. Barma (unpublished).
- [16] D. Das and M. Barma, *Phys. Rev. Lett.* **85**, 1602 (2000); D. Das, M. Barma, and S. N. Majumdar, *Phys. Rev. E* **64**, 046126 (2001); S. Chatterjee and M. Barma, *ibid.* **73**, 011107 (2006).
- [17] R. Kapri, M. Bandyopadhyay, and M. Barma, *Phys. Rev. E* **93**, 012117 (2016).

- [18] B. Derrida, E. Domany, and D. Mukamel, *J. Stat. Phys.* **69**, 667 (1992).
- [19] B. Derrida, J. L. Lebowitz, and E. R. Speer, *J. Stat. Phys.* **107**, 599 (2002).
- [20] G. E. Uhlenbeck and L. S. Ornstein, *Phys. Rev.* **36**, 823 (1930).
- [21] G. J. Bakker, C. Eich, J. A. Torreno-Pina, R. Diez-Ahedo, G. Perez-Samper, T. S. van Zanten, C. G. Figdor, A. Cambi, and M. F. Garcia-Parajo, *Proc. Natl. Acad. Sci. USA* **109**, 4869 (2012).
- [22] C. Yu, J. B. K. Law, M. Suryana, H. Y. Low, and M. P. Sheetz, *Proc. Natl. Acad. Sci. USA* **108**, 20585 (2011).
- [23] D. Goswami, K. Gowrishankar, S. Bilgrami, S. Ghosh, R. Raghupathy, R. Chadda, R. Vishwakarma, M. Rao, and S. Mayor, *Cell* **135**, 1085 (2008).
- [24] A. Das, A. Polley, and Madan Rao, *Phys. Rev. Lett.* **116**, 068306 (2016).
- [25] R. Varma, G. Campi, T. Yokosuka, T. Saito, and M. L. Dustin, *Immunity* **25**, 117 (2006).